



Article

Synthesis and Photophysical Evaluation of Isoleptic Pt(II) and Pd(II) Complexes Utilizing N[^]N[^]N[^] Ligands as Luminophoric Chelators with Different Ancillary Ligands

Silpa Padmakumar Sheelakumari ^{1,2,†}, María Victoria Cappellari ^{1,2,†} , María Belen Rivas Aiello ^{1,2}, Alexander Hepp ¹  and Cristian Alejandro Strassert ^{1,2,*}

¹ Institut für Anorganische und Analytische Chemie, Universität Münster, Corrensstraße 28/30, 48149 Münster, Germany

² CeNTech, CiMIC, SoN, Universität Münster, Heisenbergstraße 11, 48149 Münster, Germany

* Correspondence: ca.s@uni-muenster.de

† These authors contributed equally to this work (shared first authorship).

Abstract: We herein report on the synthesis and structural characterization, as well as on the photophysical properties, of a series of isoleptic Pt(II) and Pd(II) complexes featuring tridentate N[^]N[^]N[^] chelators as luminophores while bearing diverse ancillary co-ligands. Six new palladium complexes were synthesized using 2,6-bis(3-(*tert*-butyl/trifluoromethyl)-1*H*-1,2,4-triazol-5-yl)pyridine (^{*t*}bu or CF₃, respectively) in combination with four distinct ancillary ligands, namely: 4-aminopyridine (AmPy), 2,6-dimethylphenyl isonitrile (CNR), triphenylphosphane (PPh₃), and 1,3,5-triaza-7-phosphaadamantane (PTA). Thus, two novel Pt(II) complexes incorporating the co-ligands CNR and PTA were explored. The remaining platinum-based complexes, namely CF₃-Pt-AmPy, ^{*t*}bu-Pt-AmPy, CF₃-Pt-PPh₃, and ^{*t*}bu-Pt-PPh₃, were re-synthesized according to our previous work for a systematic comparison with their Pd(II) homologues. Thus, photophysical studies were performed in different solvents and conditions. The Pt(II) complexes demonstrated comparable or superior photophysical characteristics in toluene when compared with their solutions in liquid dichloromethane at room temperature. In contrast, the Pd(II) complexes exhibited no significant photoluminescence in dichloromethane, but a surprisingly clear emission was observed for ^{*t*}bu-Pd-AmPy, ^{*t*}bu-Pd-CNR, and ^{*t*}bu-Pd-PPh₃ in liquid toluene at room temperature. The significant differences regarding excited state lifetimes and photoluminescence quantum yields underscore the impact of solvent selection on photophysical characteristics, emphasizing the need to consider metal-ligand interactions, as well as the surrounding microenvironment, for a comprehensive interpretation of their photophysical properties. In addition, it is clear that AmPy and CNR render better luminescence efficiencies, whereas PTA is only suitable in toluene.



Citation: Sheelakumari, S.P.; Cappellari, M.V.; Rivas Aiello, M.B.; Hepp, A.; Strassert, C.A. Synthesis and Photophysical Evaluation of Isoleptic Pt(II) and Pd(II) Complexes Utilizing N[^]N[^]N[^] Ligands as Luminophoric Chelators with Different Ancillary Ligands. *Inorganics* **2024**, *12*, 58. <https://doi.org/10.3390/inorganics12020058>

Academic Editor: Ana De Bettencourt-Dias

Received: 30 November 2023

Revised: 23 January 2024

Accepted: 27 January 2024

Published: 14 February 2024

Keywords: Pt(II) and Pd(II) complexes; synthesis; structural characterization; steady-state and time-resolved photoluminescence spectroscopy

1. Introduction

The excited-state properties of heavy transition metal complexes render them useful for organic light-emitting diodes, molecular bioimaging, and photodynamic therapy, among other applications [1–3]. Luminescent complexes of late transition elements featuring *d*⁶, *d*⁸, and *d*¹⁰ electronic configurations present ultra-fast intersystem crossing rates, microsecond-range emission, and highly oxygen-sensitive phosphorescence in the visible part of the electromagnetic spectrum with up to 100% singlet oxygen quantum yields [4,5]. Among them, luminescent platinum complexes have gained widespread attention due to their applications in the broad fields of optoelectronics [6–8] and biology [9,10]. Notably, Pt(II) complexes have found use as antineoplastic drugs and as contrast agents in bioimaging [11,12].



Copyright: © 2024 by the authors. Licensee MDPI, Basel, Switzerland. This article is an open access article distributed under the terms and conditions of the Creative Commons Attribution (CC BY) license (<https://creativecommons.org/licenses/by/4.0/>).

Pt(II) ions possess a d^8 electronic configuration and predominantly adopt square-planar coordination environments. Several studies have focused on the coordination of tridentate ligands and transition metals to form pincer-type complexes. This structure provides enhanced stability to coordination compounds against biochemical and ligand exchange reactions, while combining the properties of metal centers with organic scaffolds [13,14]. Highly luminescent coordination compounds have been achieved with the use of bidentate [15–19] and tridentate ligands [20–22], enhancing their applicability in diverse fields. As the rigidity and the chelate effect increase, the non-radiative deactivation is reduced, thus resulting in higher photoluminescence quantum yields and longer lifetimes [23,24]. Furthermore, neutral Pt(II) complexes featuring luminophoric N \wedge N \wedge N chelators can be used as triplet emitters, with potential for blue electroluminescent devices [25]. Their substitution pattern plays a crucial role in determining whether Pt(II) or Pd(II) complexes are able to support monomeric ligand-centered triplet states ($^3\text{MP-LC}$). These emissive states are described as admixtures of ^3LC (ligand-centered states, i.e., π - π^* configurations) and $^3\text{MLCT}$ (metal-to-ligand charge-transfer states, i.e., d - π^* configurations), which has been extensively documented for Pt(II) derivatives [26,27]. Additionally, Pt(II) complexes are noteworthy for their tendency to aggregate both in solids and solutions, leading to a red-shifted phosphorescence [28]. The self-assembly of luminescent alkynylplatinum(II) terpyridyl complexes has been comprehensively documented by Yam et al. [29]. The formation of metallo-gels, characterized by a low critical gelation concentration, is attributed to both π - π and Pt \cdots Pt interactions, resulting in highly efficient aggregation [30]. Lo and Yam, among others, have leveraged the self-assembling properties of luminescent Pt(II) complexes in biosensing applications [31]. In a similar approach, Ruiz et al. have elucidated the self-assembly mechanism of Pt(II) complexes for the specific recognition of AT-rich DNA sequences, showcasing the versatile applications of this approach in molecular recognition [32].

While luminescent Pt(II) complexes are extensively available and used, their Pd(II) counterparts have been rarely explored. Their sparse representation in bibliographic literature can be attributed to the lower ligand-field splitting associated with Pd(II), due to the less diffuse nature of $4d$ orbitals when compared with the $5d$ counterparts in Pt(II) [33]. Consequently, Pd(II) complexes allow for the thermal accessibility of ligand-to-metal charge-transfer or metal-centered states (LMCT or MC, i.e., π/d - d^* configurations), leading to the population of the antibonding $d_{x^2-y^2}$ orbitals. This often results in non-radiative deactivation pathways through excited state distortion and conical intersections with the ground state. As a result, Pd(II) complexes generally show inferior luminescence efficiencies when compared with their Pt(II) analogues [34].

Despite the structural similarities between Pt(II) and Pd(II) complexes, their ligand exchange rates exhibit significant differences. Pd(II) complexes are reported to be more reactive than Pt(II) complexes in analogous environments [35]. Besides the fact that both Pt(II) and Pd(II) complexes exhibit interesting photophysical and photochemical characteristics, these properties can be fine-tuned by modifying the chelating unit or the ancillary ligands [36]. The organic ligand's rigidity, combined with the square planar coordination geometry around the metal center, hinders competitive radiationless decay pathways. The use of anionic heteroaromatic ligands in the design of luminescent Pt(II) and Pd(II) complexes has gained considerable attention in this regard [37,38]. These ligands are favoured for their ability to impart structural rigidity, to establish a strong ligand field splitting, and to provide luminescent excited states [39,40]. Additionally, the nature of the monodentate ancillary ligand occupying the remaining coordination site on the metal center assumes a pivotal role in influencing solid-state aggregation and the support of intermolecular interactions within these coordination compounds [41].

Our previous work focussed on neutral platinum(II) complexes with the N \wedge N \wedge N chromophoric ligand motif, as initially introduced by Strasser, De Cola et al. [25,42,43]. These photoactive chelators exhibit notable attributes, including a strong ligand field splitting that precludes a fast thermal population of dissociative metal-centered states,

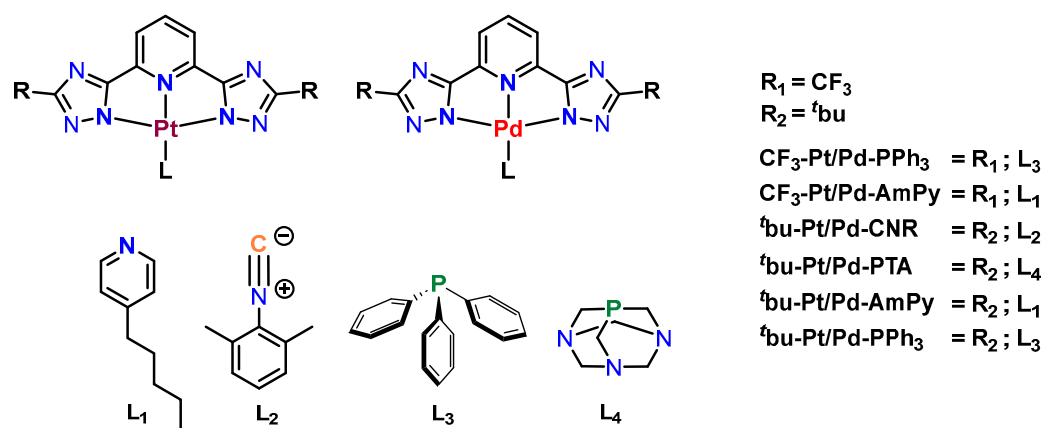
thereby minimizing radiationless deactivation processes. Building upon these prior findings, we herein employed two established luminescent chelators, namely 2,6-bis(3-(*tert*-butyl/trifluoromethyl)-1*H*-1,2,4-triazol-5-yl)pyridine, in combination with a broad range of ancillary ligands such as **AmPy**, **CNR**, **PPh₃**, and **PTA**. This approach led to a series of isoleptic platinum(II) and palladium(II) complexes, with Pt(II) and Pd(II) centers serving as perturbative metal ions.

The main objective of this work is to assess how the choice of d^8 -coordinated metal centers influences the photophysical properties when exposed to two different solvents at room temperature (DCM and toluene) and at 77 K in frozen glassy matrices (DCM/MeOH at a 1:1 volume ratio). A comprehensive range of photophysical properties were examined, including photoluminescence quantum yields (Φ_L), phosphorescence lifetimes (τ), as well as radiative and radiationless deactivation rate constants (k_r and k_{nr} , respectively).

2. Results and Discussion

2.1. Design, Synthesis, Purification, and Structural Characterization

The synthesis and characterization of a series of platinum(II) complexes, including **CF₃-Pt-AmPy**, **^tbu-Pt-AmPy**, **CF₃-Pt-PPh₃**, and **^tbu-Pt-PPh₃**, were carried out by optimizing previously established methodologies [25]. In order to ensure reproducibility and internal consistency, these Pt(II) complexes were freshly prepared, thoroughly purified and comprehensive characterization studies were carried out. To close the coordination sphere, a variety of ancillary ligands were explored. Planar **AmPy** and **CNR** ligands possessing conjugated π -systems [44] were chosen. Since complexes with planar ligands tend to form aggregates, phosphane-based ligands such as **PPh₃** and **PTA** were utilized as bulky units. Notably, **PTA** has been frequently employed in the development of anticancer complexes in previous studies [11]. The incorporation of N[^]N[^]N ligands featuring 1,2,4-triazoles with trifluoromethyl (**CF₃**) or *tert*-butyl (**^tbu**) moieties at the C3 position of the triazolato unit allowed for the fine-tuning of emission and aggregation properties (Scheme 1).



Scheme 1. Structural formulae and abbreviations of the complexes investigated herein.

Two novel platinum(II) complexes, namely **^tbu-Pt-CNR** and **^tbu-Pt-PTA**, were synthesized using a reaction mixture comprising the metal salt $\text{K}_2[\text{PtCl}_4]$, the chelating N[^]N[^]N ligand precursor, and the respective monodentate ancillary units. The synthesis involved overnight reflux in a THF-H₂O mixture for **^tbu-Pt-CNR** and in an acetonitrile (MeCN)/H₂O mixture for **^tbu-Pt-PTA**. The corresponding isoleptic Pd(II) complexes **CF₃-Pd-AmPy**, **^tbu-Pd-AmPy**, **^tbu-Pd-CNR**, **CF₃-Pd-PPh₃**, **^tbu-Pd-PPh₃**, and **^tbu-Pd-PTA** were obtained by replacing the platinum(II) salt with palladium(II) acetate ($\text{Pd}(\text{OAc})_2$). The reactions were conducted in 2-ethoxyethanol at 70 °C for **CF₃-Pd-AmPy**, **^tbu-Pd-AmPy**, and **^tbu-Pd-CNR**, whereas **CF₃-Pd-PPh₃** and **^tbu-Pd-PPh₃** required a THF-H₂O mixture; finally, **^tbu-Pd-PTA** was synthesized in MeCN-H₂O.

A detailed description of the reaction conditions, purification methods, ^1H , ^{13}C , ^{19}F , ^{31}P -, and ^{195}Pt NMR spectroscopy, as well as mass spectrometric characterization can be found in the Supplementary Materials (S02, S14, and S41).

2.2. Photophysical Characterization

All the complexes were characterized in terms of UV-visible absorption, steady-state and time-resolved photoluminescence (PL) spectroscopies, including absolute photoluminescence quantum yields (Φ_{L}) and the estimation of average radiative and radiationless deactivation rate constants. The photophysical properties were measured in diluted ($c \approx 1 \times 10^{-5}$ M) solutions in DCM or in toluene at RT, as well as in frozen glassy matrices at 77 K (DCM/MeOH, 1:1). Interestingly, the Pd(II) complexes were comparatively less soluble in toluene than their Pt(II) counterparts, which is attributed to the weaker polarizability of the Pd(II) center when compared to Pt(II) [45]. The photophysical data are summarized in Tables 1 and 2.

UV-vis absorption spectroscopy: The UV-visible absorption spectra of the Pt(II) and Pd(II) complexes show bands in the range from 230 nm to 450 nm (Figure 1 depicts the absorption spectra in DCM; the data in toluene are available in the Supplementary Materials, see Figure S78). According to bibliographic literature, the intense high-energy absorption bands can be assigned to spin-allowed transitions into ^1LC states primarily involving the tridentate ligand [46]. In addition, the energetically lower bands between 350 nm and 450 nm are assigned to transitions involving $^1\text{MLCT}$ and intra-ligand states [25]. However, it is noteworthy that the absorption bands are insensitive to the solvent's polarity. This observation can be attributed to the primary LC character of the excited states, which have dipole moments resembling the ground state [47].

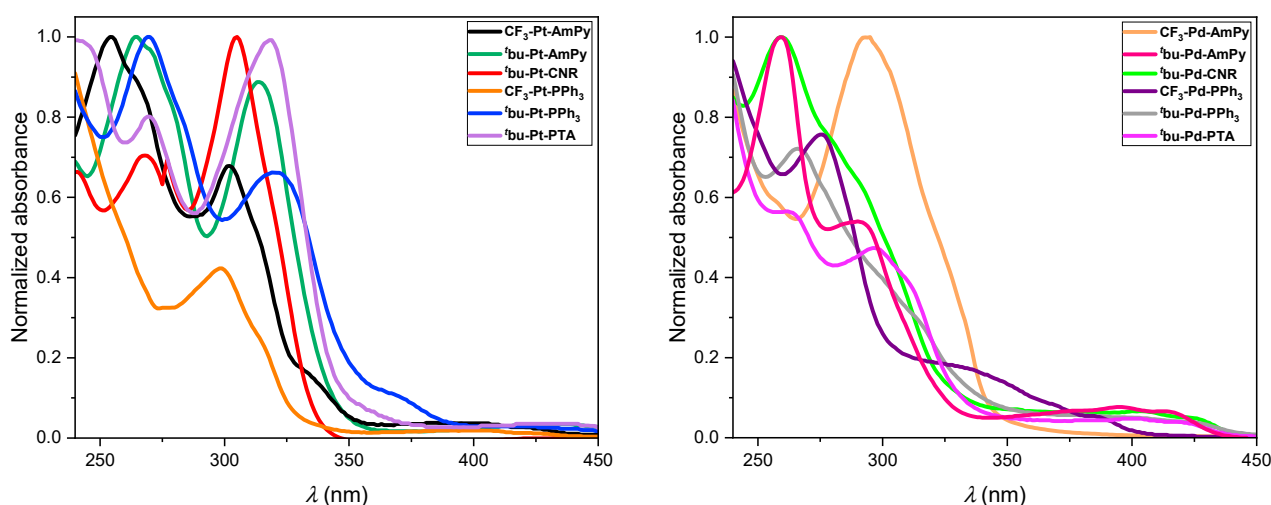


Figure 1. Normalized absorption spectra of the Pt(II) complexes (left) and Pd(II) complexes (right) in liquid DCM at RT. The molar absorption coefficients can be found in Table 1.

Time-resolved and steady-state photoluminescence spectroscopy: All compounds were characterized as liquid solutions in DCM and in toluene at RT; the corresponding emission spectra are shown in Figure 2. In both solvents, all compounds exhibited a well-defined emission spectrum showing the characteristic vibrational progression of complexes emitting from mainly ligand-centered states [22,48]. In DCM, $^t\text{Bu-Pt-AmPy}$, $^t\text{Bu-Pt-CNR}$, $^t\text{Bu-Pt-PPh}_3$, and $^t\text{Bu-Pt-PTA}$ show emission maxima peaking between 510 nm–517 nm, with photoluminescence quantum yields of 79%, 69%, <2%, and 20%, respectively (Figure 2A). $\text{CF}_3\text{-Pt-AmPy}$ shows a hypsochromic shift of the emission when compared with the other Pt(II) complexes, along with a decreased efficiency. This is attributed to the introduction of an electron-withdrawing group, which stabilizes the highest occupied molecular orbital (HOMO), leading to a blue-shifted emission where the consequently

high-lying excited state enables the thermal population of dark MC states [49]. Thus, this complex exhibits lower emission intensities, with a photoluminescence quantum yield that falls below the experimental uncertainty. No photoluminescence was detected for **CF₃-Pt-PPh₃** and for the Pd(II) complexes in liquid DCM solutions at RT, however.

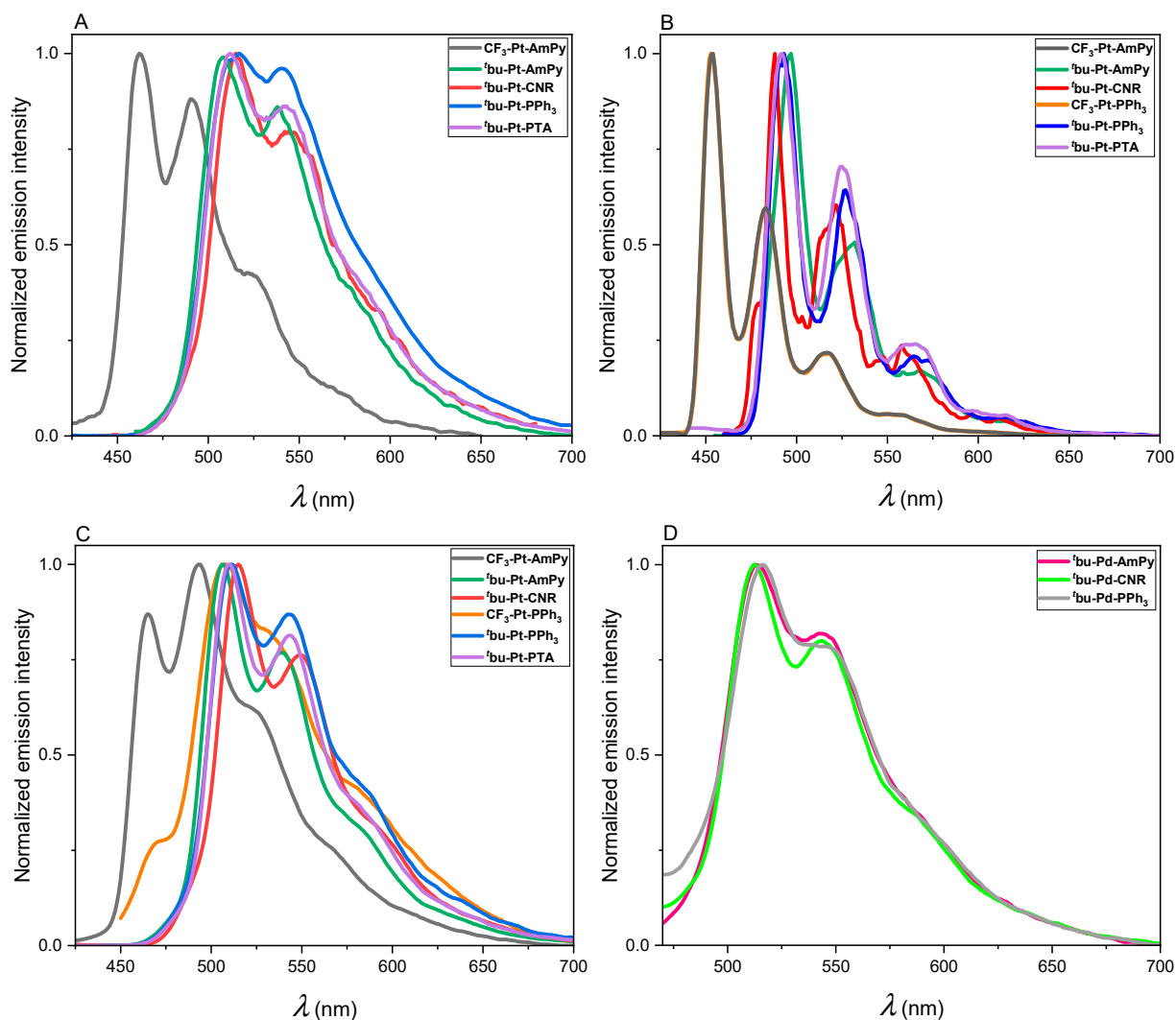


Figure 2. Photoluminescence emission spectra: (A) **CF₃-Pt-AmPy**, ^t**bu-Pt-AmPy**, ^t**bu-Pt-CNR**, ^t**bu-Pt-PPh₃**, and ^t**bu-Pt-PTA** in liquid DCM at RT (λ_{exc} ranges between 320 nm and 350 nm); (B) **CF₃-Pt-AmPy**, ^t**bu-Pt-AmPy**, ^t**bu-Pt-CNR**, **CF₃-Pt-PPh₃**, ^t**bu-Pt-PPh₃**, and ^t**bu-Pt-PTA** at 77 K in frozen glassy matrices (DCM/MeOH 1:1, λ_{exc} ranges between 300 nm and 355 nm); (C) **CF₃-Pt-AmPy**, ^t**bu-Pt-AmPy**, ^t**bu-Pt-CNR**, **CF₃-Pt-PPh₃**, ^t**bu-Pt-PPh₃**, and ^t**bu-Pt-PTA** in liquid toluene at RT (λ_{exc} ranges between 320 nm and 355 nm); (D) ^t**bu-Pd-AmPy**, ^t**bu-Pd-CNR**, and ^t**bu-Pd-PPh₃** in liquid toluene at RT (λ_{exc} ranges between 320 nm and 350 nm). The spectra are normalized to the highest intensity ($c \approx 1 \times 10^{-5}$ M).

In liquid toluene at RT, **CF₃-Pt-AmPy**, ^t**bu-Pt-AmPy**, ^t**bu-Pt-CNR**, ^t**bu-Pt-PPh₃**, and ^t**bu-Pt-PTA** show emission maxima peaking between 507 nm and 517 nm, comparable to those observed in DCM (see Figure 2C). The observed Φ_{L} values in toluene were <2%, 89%, 77%, <2%, and 85%, respectively. In a comparative analysis, these Φ_{L} either remained consistent, as in the case of **CF₃-Pt-AmPy** and ^t**bu-Pt-PPh₃**, or experienced substantial increases when compared with DCM. Even though the Pt(II) complexes exhibit a clear luminescence in both DCM and toluene at room temperature, a better resolved vibrational progression is discernible in toluene when compared with DCM. This phenomenon could

be attributed to the weaker interaction of toluene with the excited state (as opposed to the more polar to DCM), which also diminishes the values of k_{nr} . As shown in Tables 1 and 2, when toluene was used as the solvent instead of DCM, the k_r values were nearly invariant, whereas the k_{nr} values dropped (especially when PTA is used). This solvent-related effect can also account for the fact that a sizeable emission in toluene is observed for **CF₃-Pt-PPh₃** and for the Pd(II) complexes featuring *tert*-butyl substituents at the main luminophore (**^tbu-Pd-AmPy**, **^tbu-Pd-CNR**, and **^tbu-Pd-PPh₃**).

Table 1. Selected photophysical data for the Pt(II) complexes in liquid DCM at RT and in frozen glassy matrices of DCM/MeOH 1:1.

Compound	λ_{abs}/nm		RT-DCM					77 K-DCM/MeOH	
	$\epsilon/L \text{ mol}^{-1} \text{ cm}^{-1}$	λ_{em}/nm	$\tau_{Ar}/\mu s^a$	$\tau_{Air}/\mu s^a$	$\Phi_L (\%)^b$	$k_r/10^4 \text{ s}^{-1c}$	$k_{nr}/10^4 \text{ s}^{-1c}$	λ_{em}/nm	$\tau/\mu s$
CF₃-Pt-AmPy	302 (14,189) 254 (20,915)	462	0.179 ± 0.004^e	0.144 ± 0.006^e	<0.02	$k_r < 30$	$485 < k_{nr} < 498$	454	8.73 ± 0.02^e
^tbu-Pt-AmPy	314 (22,333) 265 (25,162)	510	12.44 ± 0.02^d	0.4069 ± 0.0005^d	0.79 ± 0.04	6.3 ± 0.3	1.7 ± 0.3	496	6.64 ± 0.02^e
^tbu-Pt-CNR	309 (27,625)	515	13.7 ± 0.3^d	0.374 ± 0.003^d	0.69 ± 0.03	5.0 ± 0.3	2.3 ± 0.2	487	16.75 ± 0.02^e
CF₃-Pt-PPh₃	298 (17,684)	-	-	-	-	-	-	455	14.01 ± 0.02^d
^tbu-Pt-PPh₃	321 (13,569) 270 (20,523)	517	4.88 ± 0.07^e	0.23 ± 0.01^e	<0.02	$k_r < 1$	$21 < k_{nr} < 22$	495	13.94 ± 0.04^e
^tbu-Pt-PTA	318 (12,252) 270 (9893)	512	3.819 ± 0.003^d	0.408 ± 0.003^d	0.20 ± 0.02	5.2 ± 0.9	21 ± 1	490	15.70 ± 0.02^d

^a For multi-exponential decays, the amplitude-weighted average lifetimes (τ_{av_amp}) are reported. ^b Quantum yields were measured in Ar-purged solutions. ^c The average rate constants were estimated according to $k_r = \Phi_L / \tau$ and $k_{nr} = (1 - \Phi_L) / \tau$ employing amplitude-weighted average lifetimes, as recommended by Engelborghs et al. [50]. ^d Mono-exponential decays. ^e Bi-exponential decays.

These otherwise non-emissive complexes manifested a distinct emission spectrum with a well-defined vibrational progression in toluene (see Figure 2D). Conversely, the Pd(II) complexes bearing a CF₃-substituent at the main ligand (**CF₃-Pd-AmPy**, **CF₃-Pd-PPh₃**) do not exhibit any emission under any circumstance. Thus, it is clear that the electron-donating capacity of the ^tbu-moieties resulted in a marked improvement in emission efficiency, as opposed to those with the electron-withdrawing CF₃-groups exhibiting a significantly faster nonradiative decay. This could be attributed to an elevation in the HOMO-LUMO gap with CF₃, bringing the excited state in energetic proximity to dark MC states and rendering them thermally accessible with consequently increased k_{nr} values [25]. In addition, the radiative decay (k_r) is diminished due to a weaker spin-orbit coupling for Pd(II). Thus, complexes with electron-withdrawing groups, particularly those containing a Pd(II) center, displayed lower emission efficiencies. Surprisingly, **^tbu-Pd-PTA** does not show any significant emission, not even in toluene.

The emission spectra of **CF₃-Pt-AmPy**, **^tbu-Pt-AmPy**, **^tbu-Pt-CNR**, **CF₃-Pt-PPh₃**, **^tbu-Pt-PPh₃**, and **^tbu-Pt-PTA** at 77 K are shown in Figure 2B. The Pt(II) complexes exhibited a spectrum with well-defined vibrational progressions and excited-state lifetimes in the microsecond range (6.64–16.75 μs). The luminescence can be primarily attributed to triplet LC states with a perturbative MLCT character enabling the phosphorescence, which can be described as a metal-perturbed ligand-centered (³MP-LC) character.

Furthermore, in a rigid glassy environment at low temperatures, all the complexes exhibited hypsochromic shifts of their emission bands with respect to their maxima at RT. This rigidochromic effect indicates a reduction in the MLCT character, as the reorientation of the solvent dipoles is restricted [51]. In frozen matrices at 77 K, the Pd(II) complexes showed no measurable emission, most likely due to the reduced MLCT character, which, along a weaker spin-orbit coupling (when compared with their Pt(II) counterparts), hampers the radiative deactivation. Thus, as the emission process mostly relies on ligand-centered (LC) states, and given the inherently weaker spin-orbit coupling, the relaxation of the excited state predominantly occurs by non-radiative pathways.

Table 2. Selected photophysical data for Pt(II) and Pd(II) complexes in liquid toluene at RT.

Compound	$\lambda_{\text{abs}}/\text{nm}$		RT-Toluene				
	$\epsilon/\text{L mol}^{-1} \text{ cm}^{-1}$	$\lambda_{\text{em}}/\text{nm}$	$\tau_{\text{Ar}}/\mu\text{s}^{\text{a}}$	$\tau_{\text{Air}}/\mu\text{s}^{\text{a}}$	$\Phi_{\text{L}} (\%)^{\text{b}}$	$k_{\text{r}}/10^4 \text{ s}^{-1}^{\text{c}}$	$k_{\text{nr}}/10^4 \text{ s}^{-1}^{\text{c}}$
CF ₃ -Pt-AmPy	303 (15,738)	493	6.30 ± 0.05 ^e	0.0181 ± 0.0005 ^e	<0.02	$k_{\text{r}} < 0.33$	14.8 < $k_{\text{nr}} < 15.1$
^t bu-Pt-AmPy	313 (62,145)	507	10.54 ± 0.01 ^d	0.1843 ± 0.0001 ^d	0.89 ± 0.04	8.4 ± 0.4	1.0 ± 0.4
^t bu-Pt-CNR	307 (18,168)	515	10.72 ± 0.02 ^d	0.258 ± 0.001 ^e	0.77 ± 0.04	7.2 ± 0.2	2.1 ± 0.2
CF ₃ -Pt-PPh ₃	300 (20,782)	507	5.62 ± 0.07 ^f	0.42 ± 0.01 ^e	<0.02	$k_{\text{r}} < 0.39$	17 < $k_{\text{nr}} < 18$
^t bu-Pt-PPh ₃	287 (20,664) 317 (18,213)	511	2.77 ± 0.04 ^f	1.11 ± 0.06 ^f	0.11 ± 0.02	4.0 ± 0.9	32.1 ± 0.9
^t bu-Pt-PTA	320 (11,146)	510	12.21 ± 0.02 ^d	0.170 ± 0.001 ^e	0.85 ± 0.04	7.0 ± 0.2	1.2 ± 0.2
^t bu-Pd-AmPy	295 (15,632) 399 (2041)	513	3.59 ± 0.04 ^e	0.00382 ± 0.00004 ^f	<0.02	$k_{\text{r}} < 1.18$	29 < $k_{\text{nr}} < 30$
^t bu-Pd-CNR	282 (19,473) 412 (1863)	512	7.85 ± 0.02 ^d	0.0025 ± 0.0001 ^f	<0.02	$k_{\text{r}} < 0.55$	12 < $k_{\text{nr}} < 13$
^t bu-Pd-PPh ₃	289 (29,241)	516	5.1 ± 0.2 ^e	0.00228 ± 0.00004 ^f	<0.02	$k_{\text{r}} < 0.43$	19 < $k_{\text{nr}} < 20$

^a For multi-exponential decays, the amplitude-weighted average lifetimes ($\tau_{\text{av-amp}}$) are reported. ^b Quantum yields were measured in Ar-purged solutions. ^c The average rate constants were estimated according to $k_{\text{r}} = \Phi_{\text{L}}/\tau$ and $k_{\text{nr}} = (1 - \Phi_{\text{L}})/\tau$ employing amplitude-weighted average lifetimes, as recommended by Engelborghs et al. [50]. ^d Mono-exponential decays. ^e Bi-exponential decays. ^f Tri-exponential decays.

3. Methods and Materials

Materials: All commercially available chemicals and solvents were used as purchased. For the purification of the ligand precursors and complexes, silica gel 60 from Merck was used as the stationary phase in column-chromatographic separations.

Synthesis: A detailed description of the synthesis (experimental procedures, reaction conditions, and purification methods) can be found in the Supplementary Materials.

Structural characterization: All compounds were characterized by 1D-NMR experiments (¹H, ¹³C, ¹³C{¹H} DEPT135, and ¹⁹⁵Pt) and 2D-NMR experiments (HH-COSY, HC-HSQC, HC-HMBC). The NMR spectra were recorded at the Institut für Anorganische und Analytische Chemie (Universität Münster) using a Bruker Avance III 400, Bruker Avance Neo 400, or a Bruker Avance Neo 500. All NMR measurements were performed at 300 K. The chemical shifts (δ) of the spectra are given in parts per million (ppm). The signals are referenced to the residual proton signal in the corresponding deuterated solvents: DCM-*d*₂ (¹H = 5.32 ppm/¹³C = 54.00 ppm), methanol-*d*₄ (¹H = 3.31 ppm/¹³C = 49.00 ppm) and DMF-*d*₇ (¹H = 8.03 ppm, 2.92 ppm, 2.75 ppm/¹³C = 163.15 ppm, 34.89 ppm, 29.76 ppm). The signal multiplicities are given as s (singlet), d (doublet), t (triplet), and m (multiplet). The mass spectrometric analysis was carried out at the Institut für Anorganische und Analytische Chemie (Universität Münster) using a Bruker Impact II with electrospray ionization (ESI) to obtain exact mass (EM) spectra for all compounds. The samples were dissolved in MeOH and injected with an autosampler using a mixture of MeOH and MeCN as the solvent. The corresponding NMR spectra are presented in the Supplementary Materials, as well as the mass spectra for all compounds (see Figures S1–S77).

Photophysical characterization: All metal complexes were analyzed by steady-state and time-resolved photoluminescence spectroscopy. Absorption spectra were measured with a Shimadzu UV-1900i UV-VIS-NIR spectrophotometer. All the solvents used were of spectrometric grade (Uvasol®). Photoluminescence quantum yields were measured using a Hamamatsu Photonics absolute PL quantum yield measurement system (C9920-02) equipped with a L9799-01 CW Xe light source (150 W), a monochromator, a C7473 photonic multi-channel analyzer, and an integrating sphere while employing the U6039-05 software (Hamamatsu Photonics, Ltd., Shizuoka, Japan).

Steady-state excitation and emission spectra were recorded on a FluoTime 300 spectrometer from PicoQuant equipped with a 300 W ozone-free Xe lamp (250–900 nm), a 10 W Xe flashlamp (250–900 nm, pulse width ca. 1 μs) with repetition rates of 0.1–300 Hz, a double-grating excitation monochromator (Czerny-Turner type, grating with 1200 lines/mm, blaze wavelength: 300 nm), diode lasers (pulse width < 80 ps) operated by a computer-controlled laser driver PDL-828 “Sepia II” (repetition rate up to 80 MHz,

burst mode for slow and weak decays), two double-grating emission monochromators (Czerny-Turner, selectable gratings blazed at 500 nm with 2.7 nm/mm dispersion and 1200 lines/mm, or blazed at 1200 nm with 5.4 nm/mm dispersion and 600 lines/mm) with adjustable slit width between 25 μm and 7 mm, and Glan-Thompson polarizers for excitation (after the Xe-lamps) and emission (after the sample). A sample holder with a Peltier-cooled mounting unit ranging from -15 to 110 $^{\circ}\text{C}$, along with two detectors (namely a PMA Hybrid-07 from PicoQuant with transit time spread FWHM < 50 ps, 200–850 nm, or a H10330C-45-C3 NIR detector with transit time spread FWHM 0.4 ns, 950–1700 nm from Hamamatsu), were used. Steady-state spectra and photoluminescence lifetimes were recorded in the TCSPC mode using a PicoHarp 300 (minimum base resolution, 4 ps) or in the MCS mode with a TimeHarp 260 (where up to several ms can be traced). Emission and excitation spectra were corrected for source intensity (lamp and grating) by standard correction curves. Lifetime analysis was performed using the commercial EasyTau 2 software (PicoQuant). The quality of the fit was assessed by minimizing the reduced chi-squared function (χ^2) and visual inspection of the weighted residuals and their autocorrelation.

4. Conclusions

In this study, we describe the synthesis and photophysical characterization of N N N-coordinated Pt(II) and Pd(II) complexes. A comparative approach was employed involving isoleptic Pt(II) and Pd(II) complexes with identical luminophoric ligands bearing either ^tbu - or CF_3 -substituents, and the auxiliary ligand was varied (including **AmPy**, **CNR**, **PPh₃**, and **PTA**). All the complexes were characterized by NMR spectroscopy and by mass spectrometry.

In general, the photophysical properties are predominantly dictated by metal-perturbed ligand-centered states. The Pt(II) complexes exhibited either similar or superior photophysical behavior in toluene compared to DCM. For the Pd(II) complexes and despite their better solubility in DCM than in toluene (yet always lower than the corresponding Pt(II) analogues), only the ^tbu -substituted compounds exhibited a measurable photoluminescence when analyzed in toluene, while they remained dark in DCM. This is attributed to a reduced interaction of toluene with the excited state, leading to a decrease of the k_{nr} values. Additionally, ^tbu -moieties destabilize the HOMO and, thereby, the energy of the emissive triplet state, which hampers radiationless deactivation paths avoiding the thermal population of dissociative MC states. At 77 K, emission was only observed for the Pt(II) complexes due to the weaker spin-orbit coupling of encountered in Pd(II) complexes when the emission arises from almost purely LC states.

Based on these results, it is clear that CF_3 -groups impair the luminescence of monomeric species at RT (as previously described in the bibliographic literature by De Cola et al. [46,52,53]), whereas the best ancillary ligands in terms of efficiency are represented by **AmPy**, which is closely followed by **CNR**. It can be observed that phosphane-based ligands (**PPh₃** and **PTA**) do not significantly affect k_r , but they do increase the k_{nr} values, resulting in lower emission efficiencies. On the other hand, it is observed that the k_{nr} value in the toluene of ^tbu -Pt-PTA is considerably lower than in DCM. This can be attributed to the dipole–dipole interactions between DCM molecules and the nitrogen atoms of the rigid **PTA** co-ligand, which is not the case in toluene. For **PPh₃** and in any solvent, the radiationless deactivation paths are rather fast, due to its bulky nature and high density of roto-vibrational degrees of freedom. Furthermore, it is interesting that toluene is able to switch on the emission of Pd(II) complexes at RT, most likely by reducing the coupling of solvent molecules with the emissive state.

Supplementary Materials: The following supporting information can be downloaded at: <https://www.mdpi.com/article/10.3390/inorganics12020058/s1>. Content: Synthesis and characterization—(S02): NMR spectroscopy—(S14): Mass spectrometry—(S41): UV-vis absorption and photoluminescence spectroscopies—(S49): References (S67).

Author Contributions: Conceptualization, S.P.S. and C.A.S.; validation, M.V.C., M.B.R.A., S.P.S. and C.A.S.; formal analysis, S.P.S., M.V.C. and M.B.R.A.; NMR measurements, A.H.; NMR structure analysis, A.H. and S.P.S.; photophysical investigation, M.V.C., M.B.R.A. and S.P.S.; resources, C.A.S.; data curation, S.P.S. and M.V.C.; writing—original draft preparation, S.P.S. and M.V.C.; writing—review and editing, S.P.S., M.V.C., M.B.R.A. and C.A.S.; visualization, S.P.S. and M.V.C.; supervision, C.A.S.; project administration, C.A.S.; funding acquisition, C.A.S. All authors have read and agreed to the published version of the manuscript.

Funding: C.A.S. gratefully acknowledges funding from the Deutsche Forschungsgemeinschaft (DFG—Collaborative Research Centre (CRC) 1450–431460824, Münster, Germany (project A02); project STR 1186/6-2 within the Priority Programme 2102 “Light-controlled reactivity of metal complexes”). C.A.S. gratefully acknowledges the generous financial support for the acquisition of an “Integrated Confocal Luminescence Spectrometer with Spatiotemporal Resolution and Multiphoton Excitation” (DFG/Land NRW: INST 211/915-1 FUGG; DFG EXC1003: “Berufungsmittel”).

Data Availability Statement: All the relevant data for this paper can be found in the article or in the Supplementary Material.

Conflicts of Interest: The authors declare no conflict of interest.

References

1. Yam, V.W.-W.; Au, V.K.-M.; Leung, S.Y.-L. Light-Emitting Self-Assembled Materials Based on D8 and D10 Transition Metal Complexes. *Chem. Rev.* **2015**, *115*, 7589–7728. [[CrossRef](#)]
2. Monro, S.; Colón, K.L.; Yin, H.; Roque, J.I.I.I.; Konda, P.; Gujar, S.; Thummel, R.P.; Lilge, L.; Cameron, C.G.; McFarland, S.A. Transition Metal Complexes and Photodynamic Therapy from a Tumor-Centered Approach: Challenges, Opportunities, and Highlights from the Development of TLD1433. *Chem. Rev.* **2019**, *119*, 797–828. [[CrossRef](#)]
3. Imberti, C.; Zhang, P.; Huang, H.; Sadler, P.J. New Designs for Phototherapeutic Transition Metal Complexes. *Angew. Chem. Int. Ed.* **2020**, *59*, 61–73. [[CrossRef](#)]
4. Zhao, Q.; Huang, C.; Li, F. Phosphorescent Heavy-Metal Complexes for Bioimaging. *Chem. Soc. Rev.* **2011**, *40*, 2508–2524. [[CrossRef](#)] [[PubMed](#)]
5. Zhao, Q.; Li, F.; Huang, C. Phosphorescent Chemosensors Based on Heavy-Metal Complexes. *Chem. Soc. Rev.* **2010**, *39*, 3007–3030. [[CrossRef](#)]
6. Sajoto, T.; Djurovich, P.I.; Tamayo, A.B.; Oxgaard, J.; Goddard, W.A.I.I.I.; Thompson, M.E. Temperature Dependence of Blue Phosphorescent Cyclometalated Ir(III) Complexes. *J. Am. Chem. Soc.* **2009**, *131*, 9813–9822. [[CrossRef](#)] [[PubMed](#)]
7. Omidyan, R.; Abbasi, M.; Azimi, G. Photophysical and Optoelectronic Properties of a Platinum(II) Complex and Its Derivatives, Designed as a Highly Efficient OLED Emitter: A Theoretical Study. *Int. J. Quantum Chem.* **2019**, *119*, e25793. [[CrossRef](#)]
8. Lamansky, S.; Djurovich, P.; Murphy, D.; Abdel-Razzaq, F.; Lee, H.-E.; Adachi, C.; Burrows, P.E.; Forrest, S.R.; Thompson, M.E. Highly Phosphorescent Bis-Cyclometalated Iridium Complexes: Synthesis, Photophysical Characterization, and Use in Organic Light Emitting Diodes. *J. Am. Chem. Soc.* **2001**, *123*, 4304–4312. [[CrossRef](#)]
9. Kobayashi, H.; Ogawa, M.; Alford, R.; Choyke, P.L.; Urano, Y. New Strategies for Fluorescent Probe Design in Medical Diagnostic Imaging. *Chem. Rev.* **2010**, *110*, 2620–2640. [[CrossRef](#)] [[PubMed](#)]
10. Mauro, M.; Aliprandi, A.; Septiadi, D.; Kehr, N.S.; De Cola, L. When Self-Assembly Meets Biology: Luminescent Platinum Complexes for Imaging Applications. *Chem. Soc. Rev.* **2014**, *43*, 4144–4166. [[CrossRef](#)]
11. Leal, J.; Durá, G.; Jalón, F.A.; Zafon, E.; Massaguer, A.; Cuevas, J.V.; Santos, L.; Rodríguez, A.M.; Manzano, B.R. Luminescent Cyclometalated Platinum Compounds with N, P, and O/O Ligands: Density-Functional Theory Studies and Analysis of the Anticancer Potential. *Appl. Organomet. Chem.* **2023**, *37*, e6983. [[CrossRef](#)]
12. Septiadi, D.; Aliprandi, A.; Mauro, M.; De Cola, L. Bio-Imaging with Neutral Luminescent Pt(II) Complexes Showing Metal···metal Interactions. *RSC Adv.* **2014**, *4*, 25709. [[CrossRef](#)]
13. Adams, R.D.; Captain, B. Bimetallic Cluster Complexes: Synthesis, Structures and Applications to Catalysis. *J. Organomet. Chem.* **2004**, *689*, 4521–4529. [[CrossRef](#)]
14. Freeman, G.R.; Williams, J.A.G. Metal complexes of pincer ligands: Excited states, photochemistry, and luminescence. In *Organometallic Pincer Chemistry*; Springer: Berlin/Heidelberg, Germany, 2013; Volume 40.
15. Williams, J.A.G. *Photochemistry and Photophysics of Coordination Compounds: Platinum BT—Photochemistry and Photophysics of Coordination Compounds II*; Balzani, V., Campagna, S., Eds.; Springer: Berlin/Heidelberg, Germany, 2007; pp. 205–268. [[CrossRef](#)]
16. Dehghanpour, S.; Mahmoudi, A.; Rostami, S. Platinum(II) Complexes with Bidentate Iminopyridine Ligands: Synthesis, Spectral Characterization, Properties and Structural Analysis. *Polyhedron* **2010**, *29*, 2190–2195. [[CrossRef](#)]
17. Luo, Z.; Liu, Y.; Tong, K.-C.; Chang, X.-Y.; To, W.-P.; Che, C.-M. Luminescent Platinum(II) Complexes with Bidentate Diacetylide Ligands: Structures, Photophysical Properties and Application Studies. *Chem.—An Asian J.* **2021**, *16*, 2978–2992. [[CrossRef](#)] [[PubMed](#)]

18. DePriest, J.; Zheng, G.Y.; Goswami, N.; Eichhorn, D.M.; Woods, C.; Rillema, D.P. Structure, Physical, and Photophysical Properties of Platinum(II) Complexes Containing Bidentate Aromatic and Bis(Diphenylphosphino)Methane as Ligands. *Inorg. Chem.* **2000**, *39*, 1955. [[CrossRef](#)] [[PubMed](#)]
19. Danilov, E.O.; Pomestchenko, I.E.; Kinayyigit, S.; Gentili, P.L.; Hissler, M.; Ziessel, R.; Castellano, F.N. Ultrafast Energy Migration in Platinum(II) Diimine Complexes Bearing Pyrenylacetylide Chromophores. *J. Phys. Chem. A* **2005**, *109*, 2465–2471. [[CrossRef](#)] [[PubMed](#)]
20. Li, Y.; Fei, Y.; Sun, H.; Yu, S.; Liu, J. Regulation of the Switchable Luminescence of Tridentate Platinum(II) Complexes by Photoisomerization. *Front. Chem.* **2021**, *8*, 2020. [[CrossRef](#)] [[PubMed](#)]
21. Haque, A.; Xu, L.; Al-Balushi, R.A.; Al-Suti, M.K.; Ilmi, R.; Guo, Z.; Khan, M.S.; Wong, W.-Y.; Raithby, P.R. Cyclometallated Tridentate Platinum(II) Arylacetylide Complexes: Old Wine in New Bottles. *Chem. Soc. Rev.* **2019**, *48*, 5547–5563. [[CrossRef](#)]
22. Hebenbrock, M.; González-Abradelo, D.; Hepp, A.; Meadowcroft, J.; Lefringhausen, N.; Strassert, C.A.; Müller, J. Influence of the Ancillary Ligands on the Luminescence of Platinum(II) Complexes with a Triazole-Based Tridentate C[∞]N[∞]N Luminophore. *Inorganica Chim. Acta* **2021**, *516*, 119988. [[CrossRef](#)]
23. Shikhova, E.; Danilov, E.O.; Kinayyigit, S.; Pomestchenko, I.E.; Tregubov, A.D.; Camerel, F.; Retaillieu, P.; Ziessel, R.; Castellano, F.N. Excited-State Absorption Properties of Platinum(II) Terpyridyl Acetylides. *Inorg. Chem.* **2007**, *46*, 3038–3048. [[CrossRef](#)] [[PubMed](#)]
24. Rausch, A.F.; Murphy, L.; Williams, J.A.G.; Yersin, H. Improving the Performance of Pt(II) Complexes for Blue Light Emission by Enhancing the Molecular Rigidity. *Inorg. Chem.* **2012**, *51*, 312–319. [[CrossRef](#)] [[PubMed](#)]
25. Sanning, J.; Ewen, P.R.; Stegemann, L.; Schmidt, J.; Daniliuc, C.G.; Koch, T.; Doltsinis, N.L.; Wegner, D.; Strassert, C.A. Scanning-Tunneling-Spectroscopy-Directed Design of Tailored Deep-Blue Emitters. *Angew. Chem. Int. Ed.* **2015**, *54*, 786–791. [[CrossRef](#)]
26. Hua, F.; Kinayyigit, S.; Cable, J.R.; Castellano, F.N. Platinum(II) Diimine Diacetylides: Metallacyclization Enhances Photophysical Properties. *Inorg. Chem.* **2006**, *45*, 4304–4306. [[CrossRef](#)]
27. Schwartz, G.; Reineke, S.; Rosenow, T.C.; Walzer, K.; Leo, K. Triplet Harvesting in Hybrid White Organic Light-Emitting Diodes. *Adv. Funct. Mater.* **2009**, *19*, 1319–1333. [[CrossRef](#)]
28. Lü, Y.; Zhang, M.; Shang, Y.; Xu, H.; Wei, B.; Wang, Z. Platinum Complexes as Phosphorescent Emitters in Highly Efficient Organic Light-Emitting Diodes. *J. Shanghai Univ. (Engl. Ed.)* **2011**, *15*, 256–261. [[CrossRef](#)]
29. Wong, K.M.-C.; Yam, V.W.-W. Self-Assembly of Luminescent Alkynylplatinum(II) Terpyridyl Complexes: Modulation of Photophysical Properties through Aggregation Behavior. *Acc. Chem. Res.* **2011**, *44*, 424. [[CrossRef](#)]
30. Yam, V.W.-W.; Wong, K.M.-C. Luminescent Metal Complexes of D6, D8 and D10 Transition Metal Centres. *Chem. Commun.* **2011**, *47*, 11579. [[CrossRef](#)]
31. Law, A.S.-Y.; Lee, L.C.-C.; Yeung, M.C.-L.; Lo, K.K.-W.; Yam, V.W.-W. Amyloid Protein-Induced Supramolecular Self-Assembly of Water-Soluble Platinum(II) Complexes: A Luminescence Assay for Amyloid Fibrillation Detection and Inhibitor Screening. *J. Am. Chem. Soc.* **2019**, *141*, 18570–18577. [[CrossRef](#)]
32. Zamora, A.; Wachter, E.; Vera, M.; Heidary, D.K.; Rodríguez, V.; Ortega, E.; Fernández-Espín, V.; Janiak, C.; Glazer, E.C.; Barone, G.; et al. Organoplatinum(II) Complexes Self-Assemble and Recognize AT-Rich Duplex DNA Sequences. *Inorg. Chem.* **2021**, *60*, 2178–2187. [[CrossRef](#)]
33. Onunga, D.O.; Bellam, R.; Mutua, G.K.; Sitati, M.; BalaKumaran, M.D.; Jaganyi, D.; Mambanda, A. Controlling the Reactivity of [Pd(II)(N[∞]N[∞]N)Cl]⁺ Complexes Using 2,6-Bis(Pyrazol-2-Yl)Pyridine Ligands for Biological Application: Substitution Reactivity, CT-DNA Interactions and in Vitro Cytotoxicity Study. *J. Inorg. Biochem.* **2020**, *213*, 111261. [[CrossRef](#)]
34. Gutierrez Suburu, M.E.; Maisuls, I.; Kösters, J.; Strassert, C.A. Room-Temperature Luminescence from Pd(II) and Pt(II) Complexes: From Mechanochromic Crystals to Flexible Polymer Matrices. *Dalton Trans.* **2022**, *51*, 13342–13350. [[CrossRef](#)] [[PubMed](#)]
35. Bugarčić, Ž.D.; Bogojeski, J.; van Eldik, R. Kinetics, Mechanism and Equilibrium Studies on the Substitution Reactions of Pd(II) in Reference to Pt(II) Complexes with Bio-Molecules. *Coord. Chem. Rev.* **2015**, *292*, 91–106. [[CrossRef](#)]
36. Drouet, S.; Paul-Roth, C.O.; Fattori, V.; Cocchi, M.; Williams, J.A.G. Platinum and Palladium Complexes of Fluorenyl Porphyrins as Red Phosphors for Light-Emitting Devices. *New J. Chem.* **2011**, *35*, 438–444. [[CrossRef](#)]
37. Zou, C.; Lin, J.; Suo, S.; Xie, M.; Chang, X.; Lu, W. Palladium(II) N-Heterocyclic Allenylidene Complexes with Extended Intercationic Pd···Pd Interactions and MMLCT Phosphorescence. *Chem. Commun.* **2018**, *54*, 5319–5322. [[CrossRef](#)]
38. Lai, S.-W.; Cheung, T.-C.; Chan, M.C.W.; Cheung, K.-K.; Peng, S.-M.; Che, C.-M. Luminescent Mononuclear and Binuclear Cyclometalated Palladium(II) Complexes of 6-Phenyl-2,2'-Bipyridines: Spectroscopic and Structural Comparisons with Platinum(II) Analogues. *Inorg. Chem.* **2000**, *39*, 255. [[CrossRef](#)] [[PubMed](#)]
39. Dalmau, D.; Urriolabeitia, E.P. Luminescence and Palladium: The Odd Couple. *Molecules* **2023**, *28*, 2663. [[CrossRef](#)] [[PubMed](#)]
40. Peris, E.; Crabtree, R.H. Key Factors in Pincer Ligand Design. *Chem. Soc. Rev.* **2018**, *47*, 1959–1968. [[CrossRef](#)]
41. Feuerstein, W.; Breher, F. Synthetic Access to a Phosphorescent Non-Palindromic Pincer Complex of Palladium by a Double Oxidative Addition—Comproportionation Sequence. *Chem. Commun.* **2020**, *56*, 12589–12592. [[CrossRef](#)]
42. Strassert, C.A.; Chien, C.-H.; Galvez Lopez, M.D.; Kourkoulos, D.; Hertel, D.; Meerholz, K.; De Cola, L. Lumineszenz Eines Platin(II)-Komplexes in Gelierenden Nanofasern Und Elektrolumineszierenden Filmen. *Angew. Chem.* **2011**, *123*, 976–980. [[CrossRef](#)]

43. Mydlak, M.; Mauro, M.; Polo, F.; Felicetti, M.; Leonhardt, J.; Diener, G.; De Cola, L.; Strassert, C.A. Controlling Aggregation in Highly Emissive Pt(II) Complexes Bearing Tridentate Dianionic N[−]N[−]N Ligands. Synthesis, Photophysics, and Electroluminescence. *Chem. Mater.* **2011**, *23*, 3659. [[CrossRef](#)]
44. Sanning, J.; Stegemann, L.; Ewen, P.R.; Schwermann, C.; Daniliuc, C.G.; Zhang, D.; Lin, N.; Duan, L.; Wegner, D.; Doltsinis, N.L.; et al. Colour-Tunable Asymmetric Cyclometalated Pt(II) Complexes and STM-Assisted Stability Assessment of Ancillary Ligands for OLEDs. *J. Mater. Chem. C* **2016**, *4*, 2560. [[CrossRef](#)]
45. Henwood, A.F.; Lesieur, M.; Bansal, A.K.; Lemaur, V.; Beljonne, D.; Thompson, D.G.; Graham, D.; Slawin, A.M.Z.; Samuel, I.D.W.; Cazin, C.S.J.; et al. Palladium(0) NHC Complexes: A New Avenue to Highly Efficient Phosphorescence. *Chem. Sci.* **2015**, *6*, 3248–3261. [[CrossRef](#)]
46. Mauro, M.; Aliprandi, A.; Cebrián, C.; Wang, D.; Kübel, C.; De Cola, L. Self-Assembly of a Neutral Platinum(II) Complex into Highly Emitting Microcrystalline Fibers through Metallophilic Interactions. *Chem. Commun.* **2014**, *50*, 7269. [[CrossRef](#)]
47. Lakowicz, J.R. (Ed.) *Principles of Fluorescence Spectroscopy*; Springer: Boston, MA, USA, 2006. [[CrossRef](#)]
48. Krause, M.; von der Stück, R.; Brünink, D.; Buss, S.; Doltsinis, N.L.; Strassert, C.A.; Klein, A. Platinum and Palladium Complexes of Tridentate −C[−]N[−]N (Phen-Idc)-Pyridine-Thiazol Ligands—A Case Study Involving Spectroelectrochemistry, Photoluminescence Spectroscopy and TD-DFT Calculations. *Inorganica Chim. Acta* **2021**, *518*, 120093. [[CrossRef](#)]
49. Gangadharappa, S.C.; Maisuls, I.; Schwab, D.A.; Kösters, J.; Doltsinis, N.L.; Strassert, C.A. Compensation of Hybridization Defects in Phosphorescent Complexes with Pnictogen-Based Ligands—A Structural, Photophysical, and Theoretical Case-Study with Predictive Character. *J. Am. Chem. Soc.* **2020**, *142*, 21353–21367. [[CrossRef](#)] [[PubMed](#)]
50. Sillen, A.; Engelborghs, Y. The Correct Use of “Average” Fluorescence Parameters. *Photochem. Photobiol.* **1998**, *67*, 475. [[CrossRef](#)]
51. Lees, A.J. The Luminescence Rigidochromic Effect Exhibited by Organometallic Complexes: Rationale and Applications. *Comments Inorg. Chem.* **1995**, *17*, 319–346. [[CrossRef](#)]
52. Carrara, S.; Aliprandi, A.; Hogan, C.F.; De Cola, L. Aggregation-Induced Electrochemiluminescence of Platinum(II) Complexes. *J. Am. Chem. Soc.* **2017**, *139*, 14605–14610. [[CrossRef](#)]
53. Aliprandi, A.; Mauro, M.; De Cola, L. Controlling and Imaging Biomimetic Self-Assembly. *Nat. Chem.* **2016**, *8*, 10–15. [[CrossRef](#)]

Disclaimer/Publisher’s Note: The statements, opinions and data contained in all publications are solely those of the individual author(s) and contributor(s) and not of MDPI and/or the editor(s). MDPI and/or the editor(s) disclaim responsibility for any injury to people or property resulting from any ideas, methods, instructions or products referred to in the content.